Multistage Stochastic Optimization for Microgrid Operation under Islanding Uncertainty

Jongheon Lee, *Student Member, IEEE,* Siyoung Lee, *Member, IEEE,* and Kyungsik Lee, *Member, IEEE*

***Abstract*—Microgrids can be distinguished from traditional power systems based on their ability to perform the islanded operation. This study explores the problem of optimizing the microgrid operation in the context of uncertain islanding events. This occurs when the microgrid is isolated from the main grid and it operates as an independent system. A multistage stochastic optimization model that considers multi-occurrence and multi-period islanding events is proposed to optimize the proactive policy. This is achieved by creating parameters for the maximum number of time periods of the islanded operation in the planning horizon. To solve the resulting large-scale mixed-integer program, an efficient algorithm based on the two-stage Benders' decomposition method is proposed. Numerical experiments show that the proposed policy significantly reduces the expected operation costs of a microgrid. This is more cost-effective in comparison to the other reactive policies that prepare a certain reserve level and reschedule the resources after an islanding event occurs. This study demonstrates that the proposed decomposition algorithm can efficiently solve large-scale problems that have longer planning horizons or a larger number of time periods for the islanded operation.**

***Index Terms*—Benders' decomposition algorithm, Islanding, Microgrid, Multistage stochastic optimization, Proactive policy.**

NOMENCLATURE

Sets and Indices:

H	Set of time periods, $t \in H = \{1, \ldots, T\}$
G	Set of thermal generation units, $g \in G$
E	Set of battery energy storage systems (BESSs), $e \in E$
S	Set of islanding scenarios, $s \in S$

Parameters:

RU_g	Ramp-up limit of unit g
RD_g	Ramp-down limit of unit g
MU_g	Minimum up time of unit g
MD_g	Minimum down time of unit g
$P_g^{\max}$	Maximum generation limit of unit g
$P_g^{\min}$	Minimum generation limit of unit g
$F_g(\cdot,\cdot)$	Generation cost function of unit g
PN_t	Total amount of renewable generation in period t
$E_e^{\max}$	Maximum storage level of BESS e
$E_e^{\min}$	Minimum storage level of BESS e
$PC_e^{\max}$	Maximum charging limit of BESS e
$PD_e^{\max}$	Maximum discharging limit of BESS e
σ_e	Changing/Discharging efficiency rate of BESS e
EN_e	Maximum number of allowed charging/discharging state changes for BESS e in the planning horizon
E_{e0}	Energy storage level of BESS e at the beginning of the planning horizon
TE_e	Target energy storage level of BESS e at the end of the planning horizon
K_t	Value of lost load (VoLL) in time period t
D_t	Load demand in time period t
R_t	System reserve requirement in time period t
ρ_t	Market price in time period t
$P_M^{\max}$	Maximum transaction amount with main grid in time period t
p_s	Probability of scenario s
τ	Maximum number of time periods of islanded operation in the planning horizon

Decision Variables:

I_{gt}^s	1 if unit g is on in time period t for scenario s, 0 otherwise
ST_{gt}^s	1 if unit g is starting up in time period t for scenario s, 0 otherwise
SP_{gt}^s	1 if unit g is shutting down in time period t for scenario s, 0 otherwise
U_{et}^s	1 if BESS e is discharging in time period t for scenario s, 0 otherwise
V_{et}^s	1 if BESS e is charging in time period t for scenario s, 0 otherwise
UV_{et}^s	1 if BESS e changes state at the beginning of time period t for scenario s, 0 otherwise
P_{gt}^s	Amount of generation of unit g in time period t for scenario s
LS_t^s	Amount of load shedding in time period t for scenario s
E_{et}^s	Energy storage level of BESS e at the end of time period t for scenario s
PC_{et}^s	Charging amount of BESS e in time period t for scenario s
PD_{et}^s	Discharging amount of BESS e in time period t for scenario s
PM_t^s	Transaction amount with the main grid in time period t for scenario s
$\mathbf{x}_c^s$	Concatenated vector of the binary variables for sce-

Manuscript received February 17, 2020; revised June 13, 2020; accepted July 12, 2020. This work was supported in part by the Korea Electric Power Corporation (Grant number: R18XA01), and in part by the Korea Institute of Energy Technology Evaluation and Planning (KETEP) grant funded by the Korea government (MOTIE) (No. 2019371010006B). Paper no. TSG-00239-2020. *(Corresponding authors: Siyoung Lee and Kyungsik Lee)*

Jongheon Lee and Kyungsik Lee are with the Department of Industrial Engineering, Seoul National University, Seoul, Korea (email: jhljg@snu.ac.kr, optima@snu.ac.kr)

Siyoung Lee is with the Department of Energy and Electrical Engineering, Korea Polytechnic University, Siheung-si, Gyeonggi-do, Korea (email: slee0519@kpu.ac.kr).

Color versions of one or more of the figures in this paper are available online at http://ieeexplore.ieee.org.

Digital Object Identifier

nario s, $(I^s_{gt}, ST^s_{gt}, SP^s_{gt})$, $\forall$ g and t

$\mathbf{x}^s_b$ Concatenated vector of the binary variables for scenario s, $(U^s_{et}, V^s_{et}, UV^s_{et})$, $\forall$ e and t

$\mathbf{x}^s_d$ Concatenated vector of the continuous variables for scenario s, $(E^s_{et}, PC^s_{et}, PD^s_{et})$, $\forall$ e and t, P^s_{gt}, $\forall$ g and t, and LS^s_t, $\forall$ t

$\mathbf{x}^s_m$ Concatenated vector of the continuous variables for scenario s, PM^s_t, $\forall$ t

I. Introduction

A microgrid is a self-operating system that consists of various distributed generators and loads with medium/low voltage distribution phases [1]. Locally distributed microgrid operators (MGOs) establish operation plans that determine the amount of power transactions with the main transmission system (main grid) as well as the amount of power produced by the generators, based on the forecasted load demand for the jurisdiction.

The ability of the islanded operation in microgrids is one of the most important features that distinguishes them from traditional power systems. The islanded operation, which occurs when the microgrid is isolated from the main grid and it operates as an independent system, can improve the reliability of a microgrid. This can be achieved by preventing external accidents from being transmitted inside. However, because a microgrid typically has a limited generation capability and it cannot receive electricity from the main grid during the islanded operation, a reliable energy supply cannot be assured unless the internal generators are properly prepared. Therefore, the MGO must consider the possibility of the islanded operation to enhance the reliability of the microgrid when establishing an operation plan.

Presently, the literature for islanding events is limited and there is little research in the context of operation planning. Some studies [2]-[4], assume that the MGO operates a microgrid with a *reactive policy* that reschedules the resources after an islanding event occurs with or without a prespecified level of reserve capacity. Meanwhile, the reliability and cost-effectiveness of a microgrid under the islanding uncertainty may be further improved over reactive policies with a *proactive policy*. This is a pre-planned baseline operation plan along with the recourse actions for each possible islanding event under consideration. There have been some studies that have focused on the proactive policy [5]-[11]. Farzin *et al.* [5] suggested an operation planning approach to minimize the cost when the duration of the islanded operation is uncertain. Khodaei [6] proposed a $T - \tau$ criterion under which each possible islanding scenario during the planning horizon of T time periods corresponds to an islanded operation during τ consecutive periods. With the $T - \tau$ criterion, the study proposed a model and a decomposition algorithm to set up a proactive policy. In addition to islanding uncertainty, the uncertain load demand and the renewable generation were also considered in [7] and [8]. An operation plan of a microgrid is set up with the help of a demand response program in [9], where the duration of an islanding event is considered to be uncertain. In addition, robust optimization approaches with budget uncertainty sets are also suggested in [10] and [11], where the duration of an islanding event is controlled by a parameter.

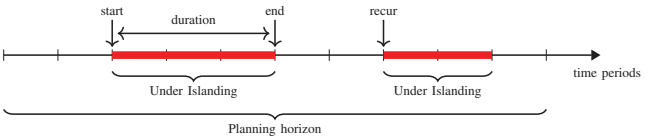

Fig. 1. Illustration of multi-occurring multi-period islanding events

Although the above-mentioned existing studies have made important contributions, a number of points need to be addressed to optimize the operation of the microgrids for the islanding events.

As previously reported, islanding events were viewed only as contingencies to avoid spreading accidents. However, because they may not be a serious inconvenience to internal loads if they are properly prepared, microgrid islanding can also be used as an ancillary service for the operation of the main grid by the system operator. There are some studies on the use of demand-side reserve resources [12]-[15]. In this regard, Lee *et al.* [16] interpreted microgrid islanding as a contract in the reserve market. In this situation, the system operator can use it as a reserve resource to improve the grid reliability. Since the reserve resources are deployed for the system operation, the number of occurrences and the duration of the islanding events during the planning horizon can vary according to the contractual relationship between the MGO and the system operator [15]. Considering that the global electricity markets are increasing their time granularity as the level of renewable energy increases [17]-[18], microgrid islanding can occur several times a day on a 15-minute or 30-minute basis. In this respect, the existing studies in the context of operation planning are limited since the proposed methods may not make the microgrids' energy supply sufficiently reliable and cost-effective. Therefore, optimizing a proactive policy that considers multi-period islanding events and multiple occurrences is necessary.

To the best of our knowledge, optimization models that consider uncertain islanding events as described in previous studies [5]-[11] are restricted to two-stage models. As a result, a normal operation plan is made in the first-stage and a set of recourse actions under the full realization of uncertain factors is made in the second-stage. However, when considering the dynamic nature of islanding events, a multistage model needs to be developed that carefully considers the *non-anticipativity* constraints. This will enforce a recourse decision without the knowledge of future islanding events. In other words, since the start, end, and the recurrence of islanding events are not known in advance, as demonstrated in Fig. 1, recourse actions made to the baseline plan up to time period t cannot be planned and executed in anticipation of the islanding events, which might occur after $t + 1$. Thus, the non-anticipativity constraints should be appropriately considered when establishing the operation plans. That is, a proactive policy can genuinely be accomplished by the multistage model with non-

anticipativity constraints, which cannot be fully achieved by two-stage models [5]-[11]. Otherwise, an operation plan can be inexecutable by itself or can incur a significant cost [19].

This paper focuses on resolving the above-mentioned issues, and the contributions are summarized as follows.

- In order to consider the recurring multi-period islanding events, a T^τ criterion is proposed. With this criterion, the islanding scenario corresponds to the islanded operations that occur up to τ for T time periods and they are not necessarily consecutive. By incorporating the possibility of the realization of each scenario by optimizing a proactive policy, the probability of each scenario is considered. Based on the T^τ criterion, a multistage stochastic optimization model is proposed to set up a proactive policy that minimizes the expectation of the total operation cost. As a result, the non-anticipativity constraint was carefully implemented to ensure the feasibility of the obtained proactive policy.
- The proposed T^τ criterion is not a minor extension of the $T-\tau$ criterion by Khodaei [6]. The number of possible islanding scenarios under the $T-\tau$ criterion is at most T; however, the T^τ criterion is $\mathcal{O}(T^\tau)$, which makes the scale of the optimization model fundamentally different. To solve this large-scale problem, an efficient algorithm was devised based on the two-stage Benders' decomposition method, which can be deployed in practice. The proposed algorithm also provides a controllable parameter to speed up the computation while guaranteeing the quality of the obtained solution to be within a pre-specified error; thus, further enhancing its practical applicability.
- Through numerical experiments, the performance of the proposed proactive policy was quantitatively evaluated and compared with the reactive policies that prepare a reserve capacity and reschedule the resources after islanding events occur. In addition, a sensitivity analysis that examines the change of the market prices or the islanding probabilities was conducted.

The rest of the paper is organized as follows. In Section II, an extensive formulation of the multistage stochastic optimization model with the related modeling considerations is presented. In Section III, an efficient algorithm based on the two-stage Benders' decomposition method is described. Section IV provides a discussion of the numerical experiments to investigate the performance of the proposed approach. Finally, Section V delivers the conclusions of this study followed by a description of our future research.

II. Multistage Stochastic Optimization Model

A. Islanding Scenarios with the T^τ criterion

The planning horizon which is typically one day is discretized into T time periods, each of whose length is typically one hour. However, it can be shorter depending on the desired granularity of operation plans. For a given integer parameter τ, $0 \le \tau \le T$, a possible islanding scenario under the T^τ criterion is any set of k time periods of islanded operation such that $k \le \tau$.

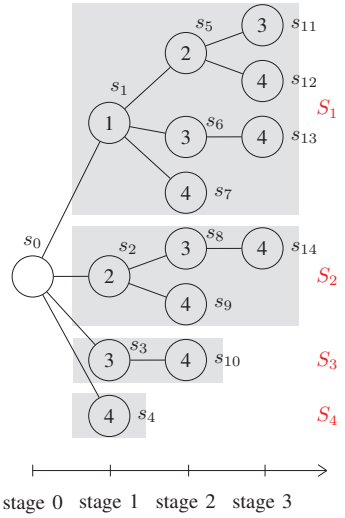

s	I_s
s_0	$\emptyset$
s_1	$\{1\}$
s_2	$\{2\}$
s_3	$\{3\}$
s_4	$\{4\}$
s_5	$\{1,2\}$
s_6	$\{1,3\}$
s_7	$\{1,4\}$
s_8	$\{2,3\}$
s_9	$\{2,4\}$
s_{10}	$\{3,4\}$
s_{11}	$\{1,2,3\}$
s_{12}	$\{1,2,4\}$
s_{13}	$\{1,3,4\}$
s_{14}	$\{2,3,4\}$

Fig. 2. Scenario tree ($T=4$, $\tau=3$) and a partition of $S \setminus \{s_0\}$

Let S be the set of all possible scenarios, and for each $s \in S$ let $I_s \subseteq H$ be the corresponding time periods of islanded operation. The set S can be represented in a tree structure, which we call the scenario tree, as depicted in Fig. 2 with $T=4$ and $\tau=3$. Each node of the tree represents the time period that the microgrid is under islanded operation. An islanding scenario corresponds to each node, in which a set of islanding events is represented by the path from the root node to that node. For example, scenario s_2 indicates islanding in period 2 and resynchronization with the main grid in period 3. Of course, islanded operation could last through period 3 (s_8) or period 4 (s_{14}), or recur in period 4 after resynchronization in period 3 (s_9).

B. Baseline Plan and Recourse Actions

Adjustable loads that could be curtailed, dispatchable thermal units, non-dispatchable renewable sources, and BESSs are considered as the components of a microgrid. A proactive policy consists of a baseline plan and a sequence of recourse actions (an adjustment plan) for each possible islanding scenario. A baseline plan sets up transaction amount with the main grid, commitment states of dispatchable units and the corresponding generation amount, and the amount of lost loads for each time period of the horizon for scenario s_0 that corresponds to the normal operation. Those factors can be adjusted in preparing a sequence of recourse actions for each islanding scenario, and a higher degree of freedom in the adjustment reduces the additional cost incurred by the change. However, quickly modifying the planned commitment states of thermal units may not be viable in practice. Therefore, in setting up a sequence of recourse actions for each islanding scenario, the commitment states of thermal units determined by the baseline plan for the whole planning horizon is fixed, but all the other factors are allowed to be adjusted. Note that we allow the charging/discharging states of BESSs to be modified to take advantage of the fast response characteristics of BESSs.

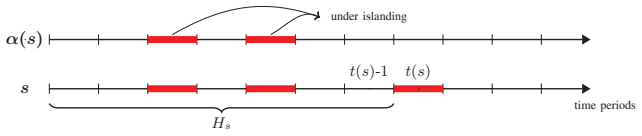

Fig. 3. Illustration of the relationship between the operation plans of scenario s and its parent $\alpha(s)$

C. Non-anticipativity Constraint

Since an MGO has no choice but to make decisions without knowing exactly which of the various future islanding scenarios will become reality, one operation plan up to time period t should be set up for a subset of scenarios each of which has the same set of time periods of islanded operation up to t. To consider this non-anticipativity constraint, relationships among the scenarios are defined and carefully handled.

For each scenario $s \in S$, let H_s be the set of time periods until just before the last islanding event, that is, $H_s := \{1, \ldots, t(s)-1\}$ where $t(s) = \max\{k | k \in I_s\}$. For $s_i, s_j \in S$, we also call s_i the *parent* scenario of s_j, which is denoted as $\alpha(s_j) = s_i$, if $I_{s_i} = I_{s_j} \cap H_{s_j}$. For example, in Fig. 2, $\alpha(s_{14}) = s_8$, $\alpha(s_8) = s_2$, and $\alpha(s_2) = s_0$. The non-anticipativity constraint means that the operation plan up to $t(s)-1$ for scenario $s \in S$ should be the same as that of its parent scenario $\alpha(s)$, as illustrated in Fig. 3, which is very important to ensure the feasibility of the operation plan.

D. Extensive Formulation of the Optimization Model

In the following, a multistage stochastic optimization model to optimize a proactive policy is proposed considering the modeling issues described earlier in this section. The model is presented in the form of the extensive formulation which will be represented in a compact formulation in the next section to describe our decomposition approach.

$$\min \sum_{s\in S} p_s \sum_{t\in H, g\in G} [F_g(P^s_{gt}, ST^s_{gt}) + \rho_t PM^s_t + K_t LS^s_t] \quad (1)$$

$$\text{s.t.} \sum_{g\in G} P^s_{gt} + \sum_{e\in E} (PD^s_{et} - PC^s_{et}) + PM^s_t + PN_t + LS^s_t \geq D_t, \quad \forall t \in H, s \in S, \quad (2)$$

$$PM^s_t = 0, \quad \forall s \in S, t \in I_s, \quad (3)$$

$$-P^{\max}_M \leq PM^s_t \leq P^{\max}_M, \quad \forall s \in S, t \in H \setminus I_s, \quad (4)$$

$$P^{\min}_g I^s_{gt} \leq P^s_{gt} \leq P^{\max}_g I^s_{gt}, \quad \forall g \in G, t \in H, s \in S, \quad (5)$$

$$P^s_{gt} - P^s_{g(t-1)} \leq RU_g, \quad \forall g \in G, t \in H, s \in S, \quad (6)$$

$$P^s_{g(t-1)} - P^s_{gt} \leq RD_g, \quad \forall g \in G, t \in H, s \in S, \quad (7)$$

$$PD^s_{et} \leq PD^{\max}_e U^s_{et}, \quad \forall e \in E, t \in H, s \in S, \quad (8)$$

$$PC^s_{et} \leq PC^{\max}_e V^s_{et}, \quad \forall e \in E, t \in H, s \in S, \quad (9)$$

$$U^s_{et} + V^s_{et} \leq 1, \quad \forall e \in E, t \in H, s \in S, \quad (10)$$

$$E^s_{et} = E^s_{e(t-1)} + \sigma_e PC^s_{et} - \frac{1}{\sigma_e} PD^s_{et}, \quad \forall e \in E, t \in H, s \in S, \quad (11)$$

$$E^{\min}_e \leq E^s_{et} \leq E^{\max}_e, \quad \forall e \in E, t \in H, s \in S, \quad (12)$$

$$E^s_{eT} = TE_e, \quad \forall e \in E, s \in S, \quad (13)$$

$$\sum_{t\in H} UV^{s_0}_{et} \leq EN_e, \quad \forall e \in E, \quad (14)$$

$$UV^{s_0}_{et} \geq U^{s_0}_{et} - U^{s_0}_{e(t-1)}, \quad \forall e \in E, t \in H, \quad (15)$$

$$UV^{s_0}_{et} \geq V^{s_0}_{et} - V^{s_0}_{e(t-1)}, \quad \forall e \in E, t \in H, \quad (16)$$

$$ST^{s_0}_{gt} \geq I^{s_0}_{gt} - I^{s_0}_{g(t-1)}, \quad \forall g \in G, t \in H, \quad (17)$$

$$SP^{s_0}_{gt} \geq I^{s_0}_{g(t-1)} - I^{s_0}_{gt}, \quad \forall g \in G, t \in H, \quad (18)$$

$$I^{s_0}_{gt} - I^{s_0}_{g(t-1)} \leq I^{s_0}_{gk}, \quad \forall k \in [t+1, \min\{t+MU_g-1, T\}], t \in H \setminus \{1\}, \quad (19)$$

$$I^{s_0}_{g(t-1)} - I^{s_0}_{gt} \leq 1 - I^{s_0}_{gk}, \quad \forall k \in [t+1, \min\{t+MD_g-1, T\}], t \in H \setminus \{1\}, \quad (20)$$

$$I^s_{gt} = I^{s_0}_{gt}, \quad \forall g \in G, t \in H, s \in S, \quad (21)$$

$$ST^s_{gt} = ST^{s_0}_{gt}, \quad \forall g \in G, t \in H, s \in S, \quad (22)$$

$$SP^s_{gt} = SP^{s_0}_{gt}, \quad \forall g \in G, t \in H, s \in S, \quad (23)$$

$$P^s_{gt} = P^{\alpha(s)}_{gt}, \quad \forall g \in G, t \in H_s, s \in S \setminus \{s_0\}, \quad (24)$$

$$PM^s_t = PM^{\alpha(s)}_t, \quad \forall t \in H_s, s \in S \setminus \{s_0\}, \quad (25)$$

$$U^s_{et} = U^{\alpha(s)}_{et}, \quad \forall e \in E, t \in H_s, s \in S \setminus \{s_0\}, \quad (26)$$

$$V^s_{et} = V^{\alpha(s)}_{et}, \quad \forall e \in E, t \in H_s, s \in S \setminus \{s_0\}, \quad (27)$$

$$PC^s_{et} = PC^{\alpha(s)}_{et}, \quad \forall e \in E, t \in H_s, s \in S \setminus \{s_0\}, \quad (28)$$

$$PD^s_{et} = PD^{\alpha(s)}_{et}, \quad \forall e \in E, t \in H_s, s \in S \setminus \{s_0\}, \quad (29)$$

$$I^s_{gt}, ST^s_{gt}, SP^s_{gt}, U^s_{et}, V^s_{et}, UV^s_{et} \in \{0,1\}, \quad \forall g \in G, e \in E, t \in H, s \in S,$$

$$P^s_{gt}, LS^s_t, E^s_{et}, PC^s_{et}, PD^s_{et} \geq 0, \quad \forall g \in G, e \in E, t \in H, s \in S.$$

Objective function (1) is the expected total operation costs where p_s is the probability of scenario $s \in S$. For each scenario s, the operation costs consist of the power generation cost, power transaction cost with the main grid, and penalty cost for load shedding. The generation cost is the sum of the start-up cost and variable generation cost. For the variable generation cost of a generator, we use a linear approximation according to [6], [20]. The transaction cost is calculated by multiplying the transaction amount by the market price. When purchasing power from the main grid, the cost is positive, and in the opposite case, a negative cost (profit) is incurred. Finally, the penalty cost is calculated by multiplying the load shedding amount by the value of lost load (VoLL).

The constraints consist of operational constraints (2)-(20) and the non-anticipativity constraints (21)-(29). Constraint (2) ensures load demand should be met for each time period. Constraint (3) indicates that the microgrid cannot perform transaction with the main grid when islanding occurs, and (4) limits the amount of power that can be transferred to or from the main grid. Each unit's maximum/minimum generation limits and ramp up/down rate limits are imposed in (5)-(7). Constraints (8) and (9) limit the maximum charging and discharging values of each BESS. Constraint (10) requires that the state of each BESS in each time period is either charging or discharging. Constraint (11) defines the storage transition function of a BESS at each time period, and (12) sets the maximum and minimum energy storage levels for the safe use

of BESSs. Constraint (13) ensures that the energy storage level of each BESS must match the target at the end of the planning horizon. Constraints (14)-(20) represent operational constraints for s_0. Constraint (14) limits the number of state transitions of BESSs in the planning horizon. Constraints (15) and (16) are logical constraints placed on the charging/discharging states to represent the number of state transitions. Note that (14) is imposed only for s_0 since we allow the state of BESSs to be changed under islanded operation. Constraints (17) and (18) are defined to represent the logical relationships between on and off state and the start-up and shut-down actions. Constraints (19) and (20) impose the minimum up and down times for each unit. Constraints (21)-(29) indicate non-anticipative requirements. Constraints (21)-(23) specify that the commitment states of generators for each scenario are the same as that of s_0. Constraints (24)-(29) require that the remaining decisions of each scenario are the same as those of its parent scenario.

III. Decomposition Approach

The optimization model given in the previous section is a large-scale mixed-integer program (MIP), whose number of variables and constraints grow exponentially as T and τ get larger. For example, if $T = 24$ and $\tau = 2$, the size of the model is about 300 times larger than that with no islanding event ($\tau = 0$), so that the number of variables and that of constraints is over 170,000 for the experimental setting with four thermal generators given in the next section. This observation motivates us to devise an efficient and well-tailored decomposition algorithm based on the Benders' decomposition method [21], which is also known as the L-shaped method [22]. The proposed approach can provide an optimal solution or a provable near optimal solution in a reasonable time. This can be achieved by controlling a parameter, $\epsilon \geq 0$, which is the duality gap.

A. Compact Representation of the Extensive Formulation

For the ease of the expositions of our decomposition approach, we first represent the extensive formulation in a compact form using the concatenated vectors of decision variables, $\mathbf{x}_c^s$, $\mathbf{x}_b^s$, $\mathbf{x}_d^s$, and $\mathbf{x}_m^s$, for all $s \in S$. For that purpose, we define $S_i (\subset S)$ for each $i \in H$ as the set of scenarios for which the first islanding event occurs in period i. Then, $\{S_1, S_2, \ldots, S_T\}$ forms a partition of $S \setminus \{s_0\}$ as illustrated in Fig. 2 given earlier. We also let $\mathcal{C}$ be the dimension of $\mathbf{x}_c^s$, and let $\mathcal{B}$ be that of $\mathbf{x}_b^s$. Then, the extensive formulation can be rewritten as the following compact form where $\mathbf{x}^s := (\mathbf{x}_c^s, \mathbf{x}_b^s, \mathbf{x}_d^s, \mathbf{x}_m^s)$.

$$\min \quad p_{s_0}\mathbf{c}^\top \mathbf{x}^{s_0} + \sum_{i\in H}\sum_{s\in S_i} p_s \mathbf{c}^\top \mathbf{x}^s \tag{30}$$

$$\text{s.t.} \quad A\mathbf{x}^{s_0} \geq \mathbf{b}, \tag{31}$$

$$A^s\mathbf{x}^s \geq \mathbf{b}^\mathbf{s}, \qquad \forall s \in S_i, i \in H, \tag{32}$$

$$\mathbf{x}_c^s = \mathbf{x}_c^{s_0}, \qquad \forall s \in S_i, i \in H, \tag{33}$$

$$C^s\mathbf{x}^s = C^s\mathbf{x}^{\alpha(s)}, \quad \forall s \in S_i, i \in H, \tag{34}$$

$$\mathbf{x}_c^s \in \{0,1\}^\mathcal{C}, \mathbf{x}_b^s \in \{0,1\}^\mathcal{B}, \quad \forall s \in S,$$

$$\mathbf{x}_d^s \geq 0, \quad \forall s \in S,$$

where $\mathbf{c}$ is the cost vector of an appropriate dimension. Constraint (31) is a vector inequality representation of constraints (2)-(20) related to s_0 with a matrix A and a vector $\mathbf{b}$ of appropriate dimensions. Similarly, constraint (32) corresponds to constraints (2)-(13) related to $s \in S \setminus \{s_0\}$. Constraints (33) and (34) are the non-anticipativity constraints. Among them, constraint (33) specifies that the commitment decision of the remaining scenarios should be the same as that of s_0, which corresponds to constraints (21)-(23). Finally, constraint (34) is a compact representation of constraints (24)-(29) related to $s \in S \setminus \{s_0\}$.

B. Decomposition Algorithm

Based on the two-stage Benders' decomposition method, an efficient decomposition algorithm, BD(ϵ), is devised as given in Algorithm 1, for which we decompose the extensive formulation into one first-stage master problem, MP, and a number of second-stage subproblems, $SUB(i)$ for each $i \in H$. MP is to determine $\mathbf{x}^{s_0}$, which is the baseline operation plan for scenario s_0, while minimizing the sum of the expected cost of $\mathbf{x}^{s_0}$ and the sum of estimates (η_i) of the optimal objective values of the subproblems, so that the optimal objective value of MP gives a lower bound (z_L) on that of the extensive formulation. For the given optimal solution of MP, $\hat{\mathbf{x}}^{s_0}$ and $\hat{\eta}_i$ for all $i \in H$, $SUB(i)$ is to find $\mathbf{x}^s$ for all $s \in S_i$ while minimizing the total expected cost over all scenarios in S_i. If we further let $\hat{\mathbf{x}}^s$ for all $s \in S \setminus \{s_0\}$ be the optimal solutions obtained by solving the subproblems, then it can be readily shown that the solution $\hat{\mathbf{x}}^s$ for all $s \in S$ is feasible to the extensive formulation, and hence the corresponding objective value is a valid upper bound (z_U). If the optimal objective value of $SUB(i)$ (z^i) for each $i \in H$ is not greater than $\hat{\eta}_i$, then the current solution $\hat{\mathbf{x}}^s$ for all $s \in S$ is optimal, i.e., $z_L = z_U$. Otherwise, we find and add the so-called optimality cuts to correct the value of the estimate η_i for $i \in H$ such that $z^i > \hat{\eta}_i$, and then repeat the above process until $z_U - z_L < \epsilon z_L$ for a pre-specified control parameter $\epsilon > 0$. Now, we give the master problem and the corresponding subproblems in the $(n+1)$th iteration as follows.

$$(MP) \quad \min \quad p_{s_0}\mathbf{c}^\top \mathbf{x}^{s_0} + \sum_{i\in H}\eta_i \tag{35}$$

$$\text{s.t.} \quad A\mathbf{x}^{s_0} \geq \mathbf{b}, \tag{36}$$

$$\eta_i \geq (\mathbf{a}_i^k)^\top \mathbf{x}^{s_0} + d_i^k, \quad \forall i \in H, k \in [n], \tag{37}$$

$$\mathbf{x}_c^{s_0} \in \{0,1\}^\mathcal{C}, \mathbf{x}_b^{s_0} \in \{0,1\}^\mathcal{B}, \mathbf{x}_d^{s_0} \geq 0,$$

where $[n] := \{1, \ldots, n\}$ and constraints in (37) are the optimality cuts added up to iteration n. For each $i \in H$, the corresponding subproblem is as follows where $\hat{\mathbf{x}}^{s_0}$ is the obtained optimal solution of MP and s_i is the scenario such that $\alpha(s_i) = s_0$.

$$(SUB(i)) \quad \min \quad \sum_{s\in S_i} p_s \mathbf{c}^\top \mathbf{x}^s \tag{38}$$

$$\text{s.t.} \quad A^s\mathbf{x}^s \geq \mathbf{b}^\mathbf{s}, \quad \forall s \in S_i, \tag{39}$$

$$\mathbf{x}_c^s = \hat{\mathbf{x}}_c^{s_0}, \qquad \forall s \in S_i, \tag{40}$$

$$C^{s_i}\mathbf{x}^{s_i} = C^{s_i}\hat{\mathbf{x}}^{s_0}, \tag{41}$$

$$C^s\mathbf{x}^s = C^s\mathbf{x}^{\alpha(s)}, \quad \forall s \in S_i \setminus \{s_i\}, \quad (42)$$
$$\mathbf{x}_b^s \in \{0,1\}^{\mathcal{B}}, \mathbf{x}_d^s \geq 0, \quad \forall s \in S_i.$$

$SUB(i)$ is a mixed integer program in which the operation plans of the scenarios are established whose first islanding occurs at i. Binary variables $\mathbf{x}_b^s$ represent the charging/discharging states of BESSs. The problem is always feasible, since a feasible solution can be constructed as follows. An operation plan of each scenario $s \in S_i$ is established by setting $(\mathbf{x}_c^s, \mathbf{x}_b^s, \mathbf{x}_d^s, \mathbf{x}_m^s) = (\hat{\mathbf{x}}_c^{s_0}, \hat{\mathbf{x}}_b^{s_0}, \hat{\mathbf{x}}_d^{s_0}, \hat{\mathbf{x}}_m^{s_0})$ except for $PM_t^s = 0$ for its islanding periods $t \in I_s$ and constraint (2), which is included in (39), can be satisfied by load shedding LS_t^s in those periods. Moreover, even though $SUB(i)$ itself is a large-scale mixed integer program, it can be shown that we can construct a feasible solution to $SUB(i)$ with the same objective value from a feasible solution to its linear programming relaxation, denoted by $SUBLP(i)$. In other words, $\mathbf{x}_b^s \in \{0,1\}^{\mathcal{B}}$ in $SUB(i)$ is relaxed to $\mathbf{x}_b^s \in [0,1]^{\mathcal{B}}$. That is, we only have to solve $SUBLP(i)$ to optimize $SUB(i)$. If $z^i > \hat{\eta}_i$, then an optimality cut can be generated using the corresponding optimal dual solution of $SUBLP(i)$. Let $\boldsymbol{\mu}_s$, $\boldsymbol{\nu}_s$, and $\boldsymbol{\pi}_{s_i}$ be the obtained vectors of optimal dual solutions of appropriate dimensions corresponding to constraints (39), (40), and (41), respectively. Then, the coefficients of optimality cuts are computed as

$$(\mathbf{a}_i^{n+1})^\top := \boldsymbol{\pi}_{s_i}^\top C^{s_i} + \sum_{s \in S_i} \boldsymbol{\nu}_s^\top, \quad (43)$$

$$d_i^{n+1} := \sum_{s \in S_i} \boldsymbol{\mu}_s^\top \mathbf{b}^{\mathbf{s}}. \quad (44)$$

Since, for each $i \in H$, we find and add the corresponding optimality cut whenever $z^i > \hat{\eta}_i$, multiple cuts can be added to MP in one iteration. This approach is also known as the multicut version of the L-shaped method [22] which has the advantage of enhancing the speed of convergence by adding several cuts to the master problem at one iteration.

Algorithm 1 Two-stage decomposition algorithm

procedure BD(ϵ)
  $z_U \leftarrow \infty$, $z_L \leftarrow 0$;
  $\mathbf{x}^s \leftarrow \emptyset \ \forall\, s \in S$, $z^i \leftarrow \infty \ \forall\, i \in H$;
  $n \leftarrow 1$;
  while $z_U \geq z_L\ (1+\epsilon)$ **do**
    solve MP and get $\hat{\mathbf{x}}^{s_0}$, $\hat{\eta}_i, \ \forall\, i \in H$;
    $z_L \leftarrow p_{s_0}\mathbf{c}^\top \hat{\mathbf{x}}^{s_0} + \sum_{i \in H} \hat{\eta}_i$;
    for all $i \in H$ **do**
      solve $SUBLP(i)$ and get $\hat{\mathbf{x}}^s, \ \forall\, s \in S_i$;
      $z^i \leftarrow \sum_{s \in S_i} p_s \mathbf{c}^\top \hat{\mathbf{x}}^s$;
      if $z^i > \hat{\eta}_i$, then, add an optimality cut;
    end for
    if $z_U > \sum_{s \in S} p_s \mathbf{c}^\top \hat{\mathbf{x}}^s$ **then**
      $z_U \leftarrow \sum_{s \in S} p_s \mathbf{c}^\top \hat{\mathbf{x}}^s$;
      $\mathbf{x}^s \leftarrow \hat{\mathbf{x}}^s, \ \forall\, s \in S$;
    end if
    $n \leftarrow n + 1$;
  end while
return z_L, z_U, and $\mathbf{x}^s, \ \forall\, s \in S$;
end procedure

IV. Computational Analysis

A. Experimental Setting

A microgrid with four thermal units, one wind farm, and one BESS was used to analyze the performance of the proposed approach. The characteristics of thermal units and the BESS, which were scaled for microgrid environments based on [6] and [23], are given in Tables I and II, respectively. In Table I, a negative sign of the initial state of a generator indicates the duration during which the generator has been off. In the experiments, the length of each time period was set to 1h.

The load demand and market price follow the forecast data of PJM-RTO [24] for October 8, 2018, and the load forecast was scaled to fit the microgrid environment. In addition, the forecasted renewable generation was derived from [23] and also scaled. Those data for a 24h horizon are given in Table III. In addition, the maximum transaction with the main grid ($P_M^{\max}$) was set to 10 MW, the BESS can change states up to two times in the planning horizon ($EN_e = 2$), and the VoLL for each time period t (K_t) was set to 5,000 USD/MWh, according to [25] and [26]. The probability of scenario s_0 (p_{s_0}) was set to 0.9, and the islanding probability ($\sum_{s \in S \setminus \{s_0\}} p_s$) was set to 0.1 with p_s having the same probability for each $s \in S \setminus \{s_0\}$.

The basic setting mentioned above holds during the section, unless otherwise specified. All the experiments were conducted on an Intel Core 3.10 GHz processor with 16 GB of RAM using Xpress-MP 8.4 [27], which is a general-purpose MIP solver.

B. Cost Analysis

In the cost analysis, the proposed proactive policy with $\epsilon = 0$ was compared with three reactive policies: `D_0.1`, `D_0.2`, and `No_Reserve`. To establish a feasible real-time operation of the reactive policies, we mimicked an

TABLE I
Characteristics of Thermal Units

Generators	G1	G2	G3	G4
Unit Cost [$/MWh]	27.7	39.1	61.3	65.6
Min-Max Capacity [MW]	2-10	1-5	1-5	0.8-3
Min Up/Down Time [h]	3	3	3	1
Ramp Up/Down Rate [MW/h]	4	3	3	2.5
Start-up Cost [$]	50	20	20	5
Initial State [h]	5	3	-3	-1

TABLE II
Characteristics of BESS

BESS	Capacity [MWh]	Max Charging/ Discharging Power [MW]	SOC Operation Range [%]	Initial-Target SOC [%]	Charging/ Discharging Efficiency [%]
E1	10	5	10-90	50	90

TABLE III
LOAD DEMAND, MARKET PRICE, WIND GENERATION DATA

Time [h]	1	2	3	4	5	6
Load [MW]	21.91	21.43	21.12	21.00	21.14	21.63
Price [$/MWh]	26.63	23.11	21.10	20.52	20.62	25.10
Wind [MW]	5	4.88	5.09	5.25	4.75	4.62
Time [h]	7	8	9	10	11	12
Load [MW]	22.58	23.28	23.70	24.24	24.86	25.43
Price [$/MWh]	33.84	29.94	28.96	38.14	35.64	88.60
Wind [MW]	4.75	4.88	4.37	4.12	4.25	4.88
Time [h]	13	14	15	16	17	18
Load [MW]	25.96	26.43	26.79	26.96	27.00	26.94
Price [$/MWh]	51.11	61.66	94.87	104.75	74.10	104.69
Wind [MW]	5.09	5.38	5.09	4.75	4.37	4.00
Time [h]	19	20	21	22	23	24
Load [MW]	26.68	26.59	26.12	25.29	24.26	23.25
Price [$/MWh]	86.25	73.51	64.38	34.42	34.57	25.60
Wind [MW]	3.75	3.62	4.00	4.25	4.37	4.12

TABLE IV
OVERALL COST AND LOAD SHEDDING COMPARISON OF THE POLICIES FOR 1-DAY DATA

Policy		Operation Cost			Exp. of Load Shedding
		Base	Exp	Worst	[MWh / day]
Proactive		100	100.32	226.07	0.09
Reactive	D_0.2	105.81	110.92	461.57	1.62
	D_0.1	101.66	111.61	493.30	3.03
	No_Reserve	98.99	112.54	708.66	4.75

operation framework ([19] and [28]) that is commonly used in power systems. For the framework, a day-ahead baseline plan is amended with look-ahead dispatch processes when an unexpected event occurs. For each of the reactive policies, the baseline plan is established by solving an MIP which is the extensive formulation with $S = \{s_0\}$ and the following additional constraints to require the reserve requirement (R_t):

$$\sum_{g \in G} r_{gt}^{s_0} \geq R_t, \quad \forall t \in H, \tag{45}$$

$$P_{gt}^{s_0} + r_{gt}^{s_0} \leq P_g^{\max} I_{gt}^{s_0}, \quad \forall g \in G, t \in H, \tag{46}$$

where $r_{gt}^{s_0}$ is a nonnegative decision variable to represent the amount of reserve of unit $g \in G$ in time period $t \in H$. For D_0.1 and D_0.2, R_t was set to 0.1 and 0.2 times of load demand (D_t), respectively. In contrast, $R_t = 0$ for No_Reserve. Once an islanding event occurs at t', the baseline plan from t' onward is modified by solving again the above-mentioned MIP but with $R_{t'} = 0$ and the commitment state of thermal units determined by the initial baseline plan being fixed.

1) 1-day Data: Cost experiments were conducted for $T = 24$ and $\tau = 2$, where up to two hours of islanding events are considered in a 24h planning horizon. For the entire planning horizon, the total costs when no islanding occurs (Base) as well as the expected (Exp) and worst (Worst) costs over all possible scenarios under the T^τ criterion are compared in Table IV, where all costs were scaled by setting the base cost of the proactive policy (USD 15,900) to 100. The expected amount of load shedding for each policy is also summarized.

As shown in Table IV, the baseline operation cost of No_Reserve is the lowest because it does not prepare for islanding events unlike other policies. Therefore, this policy incurs significant cost increase when an islanding occurs and the expected and worst costs of this policy become the highest. For the other two reactive policies (D_0.1 and D_0.2), the policy with more reserve requirement responds better to uncertainty at the expense of increased baseline cost. On the other hand, the proposed proactive policy requires only about 1.0% increase in the baseline cost compared to No_Reserve, but the expected and worst cost were significantly reduced compared to reactive policies. This shows that the proposed proactive policy is more flexible and efficient in dealing with islanding uncertainty than reactive policies preparing reserve for every time period.

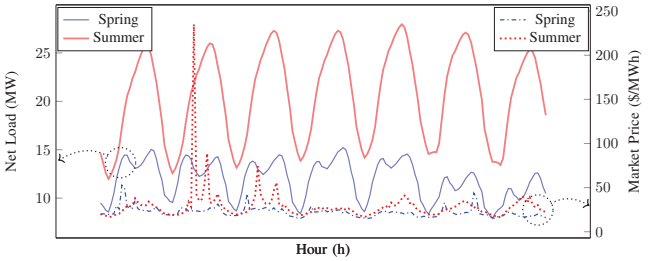

Fig. 4. Weekly net load and market price data for the spring and summer

TABLE V
OVERALL COST AND LOAD SHEDDING COMPARISON OF THE POLICIES FOR WEEKLY DATA

	Policy	Operation Cost			Exp. of Load Shedding
		Base	Exp	Worst	Ratio to Total Load (%)
Spring	Proactive	100	100.75	569.82	0.02
	D_0.2	98.97	122.47	899.87	0.80
	D_0.1	98.82	122.71	872.70	0.81
	No_reserve	97.39	147.60	1220.98	1.71
Summer	Proactive	100	100.77	299.87	0.03
	D_0.2	99.94	116.41	478.93	0.80
	D_0.1	97.92	123.18	603.21	1.23
	No_reserve	96.75	129.54	750.47	1.60

2) Weekly Data: The operation costs of our proactive policy are also compared with those of the reactive policies for different data over two weeks. This occurred during the spring off-peak period in April and during the summer peak period in July. The load demand and market price are also obtained from PJM-RTO [24], and the values of the load demand are scaled to fit our microgrid environment. In both spring and summer, the weekly wind generation data are made by repeating the values in Table III seven times. The spring and summer weekly net load and market price patterns used in this subsection are illustrated in Fig. 4, and the dotted lines indicate the market

prices. In addition, it was assumed that the islanded operation can occur up to two hours a day for each week.

The weekly operating costs of all policies in the spring and summer are represented in Table V. All costs were scaled by setting the base costs of the proactive policy in each week (Spring : USD 47,028, Summer : USD 102,634) to 100. First of all, the last column in Table V indicates the expectation of the load shedding ratio to the total load, and it is shown that load shedding barely occurs in the proactive policy even if islanding occurs. Furthermore, the result indicates that the proactive policy is more effective in spring than summer, in comparison to the other policies. This is because the low market price in the spring makes the microgrid much more dependent on the market; thus, resulting in a significant increase in the operation costs during the islanded operation. In other words, the average market price is 21.7 USD/MWh in the spring, and it is lower than the unit generation cost for all of the generators. Therefore, for the reactive policies, in which islanding events are not explicitly considered, it is efficient to set up baseline plans with purchasing as much electricity from the market as possible. In particular for `No_Reserve`, all of the thermal units are barely turned on except for the time periods where the net load exceeds the market transaction limit. On the other hand, the units are utilized more actively in the proactive policy. As a result, the proactive policy is much more efficient than the reactive policies for the expected costs and worst costs, at the expense of a small increase in the base costs.

C. Sensitivity Analysis

In the sensitivity analysis, the expected costs of the proactive policy with $\epsilon = 0$ and three reactive policies (`D_0.2`, `D_0.1`, `No_Reserve`) are compared for the 1-day data (Table III), according to the change in the market prices and islanding probabilities.

1) Market Price: A sensitivity analysis to the change in the market prices was performed. Fig. 5 shows the expected cost changes as market prices change from 0.4 to 1.6 times the base price (the market price given in Table III). The average base price (50.1 USD/MWh) is located midway between generation costs of the four generators. When the ratio is low (0.4), the market price is lower than the unit generation cost of each generator. When the ratio is high (1.6), it is more expensive than the unit cost of each generator. From Fig. 6, we can see that the expected operation costs of the proactive policy are always the lowest. On the other hand, two trends are observed for reactive policies. First, when the electricity market price is low, the operation cost of a reactive policy increases as the reserve requirement decreases. This is because lower market prices increase the amount of energy purchased from outside, which cause an increased imbalance between supply and demand in the event of islanded operation. Since microgrids are unable to handle the imbalance if they only have a small reserve capacity, expensive load shedding must be implemented. In contrast, when the electricity market price is high, the operation cost of a reactive policy decreases as the reserve requirement decreases. This is because a high reserve

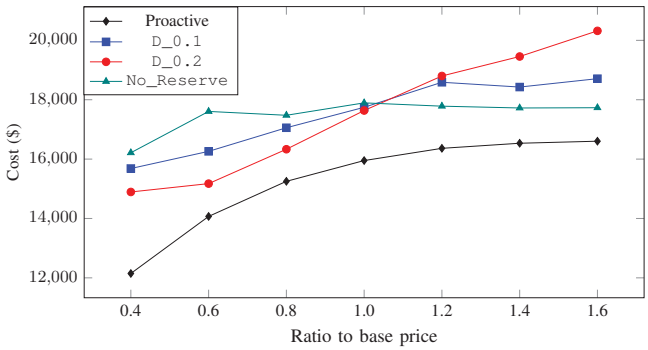

Fig. 5. Expected costs for the different electricity prices

TABLE VI
AVERAGE DEPLOYED RESERVE TO THE DEMAND RATIO(%) IN THE BASELINE PLAN

Policy	Ratio to base price						
	0.4	0.6	0.8	1.0	1.2	1.4	1.6
Proactive	25.6	27.1	22.0	17.7	11.8	8.5	6.9
`D_0.2`	22.6	26.3	25.4	24.0	22.0	21.1	20.9
`D_0.1`	13.7	14.7	13.9	13.0	10.8	12.3	12.9
`No_Reserve`	7.8	8.1	9.2	7.9	5.1	2.6	4.9

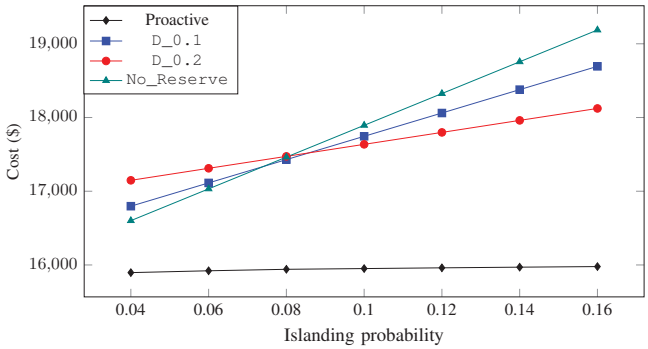

Fig. 6. Expected costs for the various islanding probabilities

requirement reduces the use of generators in the microgrid and forces it to purchase energy from the market, even though the unit price of internal generators is lower than that of the external market. That is, in this situation, the microgrid experiences a significant increase in the operation cost for the most of time periods under normal connected operation.

As Table VI shows, the proactive policy also holds considerable reserve even without explicit reserve requirements, but it varies according to the price ratio. In other words, by holding more reserve when prices are low, and less when prices are high, an MGO can be better prepared for islanding events with the proposed proactive policy than reactive policies, which hold nearly constant reserve capacities.

2) Islanding Probability: A sensitivity analysis to the change in the islanding probability was also performed. Fig. 6 shows the expected cost changes as the islanding probability ($\sum_{s \in S \setminus \{s_0\}} p_s$) varies from 0.04 to 0.16. In the experiment, the probability of each islanding scenario is set equal to each

other. From Fig. 6, a linear relationship between the islanding probability and the expected cost is shown for all policies. However, the slope of the proactive policy is the lowest, which is almost zero, and it means that the proactive policy can hedge against various islanding probabilities. Among the reactive policies, `D_0.2` is less affected than the other two reactive policies, since the slope is the lowest. This result indicates that preparing more reserve capacity is inefficient when the islanding risk is low; however, it has a critical role when the islanding risk increases. In contrast, the slope of `No_Reserve` is the highest, which implies that the policy is vulnerable when islanding is highly likely to occur.

D. Performance of Solution Approaches

The performance of our decomposition algorithm, BD(ϵ), for $\epsilon = 0, 0.01, 0.05$, and 0.1 were tested in comparison with the direct MIP approach (solving extensive formulation by an MIP solver) for different numbers of islanding scenarios and generators.

1) Different Numbers of Islanding Scenarios: The computation time of the solution approaches were compared for the different number of islanding scenarios, in which each corresponds to a combination of T and τ. Seven combinations of T and τ are tested, and the corresponding numbers of scenarios are shown in Table VII. For each combination, five instances are generated with the islanding probability ($\sum_{s\in S\setminus\{s_0\}} p_s$) being equal to 0.02, 0.04, 0.06, 0.08, or 0.1. For the instances with $T = 48$ and $T = 72$, the data set for $T = 24$ given in Table III is repeated 2 and 3 times, respectively.

TABLE VII
NUMBER OF SCENARIOS FOR THE VARIOUS T AND τ COMBINATIONS

T^τ	24^1	48^1	72^1	24^2	48^2	72^2	24^3
$\lvert S\rvert$	25	49	73	301	1,177	2,629	2,325

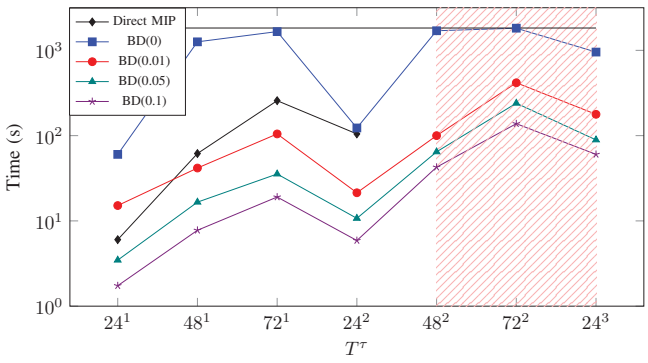

Fig. 7. Comparison of the computation time for the different numbers of scenarios

TABLE VIII
EXPECTED COST COMPARISON OF THE POLICIES IN $T = 24$ AND $\tau = 2$

Proactive Policies				Reactive Policies		
$\epsilon = 0$	$\epsilon = 0.01$	$\epsilon = 0.05$	$\epsilon = 0.1$	`D_0.2`	`D_0.1`	`No_Reserve`
100.32	100.41	100.97	100.97	110.92	111.61	112.54

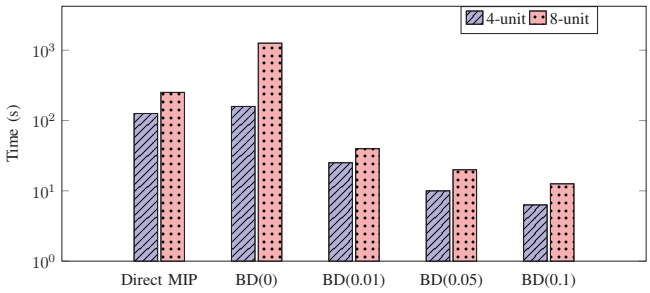

Fig. 8. Comparison of the computation time for the different numbers of generators

The average computation time over five instances of each solution approach is plotted in Fig. 7. The time limit for each instance was set to 1800s, which is indicated as the horizontal line. The red-dashed region represents the instances that could not be solved by the direct MIP approach. The results show that the direct MIP approach can be faster than BD(0) when the number of scenarios is relatively small ($24^1, 48^1$, and 72^1). However, the instances with larger numbers of scenarios ($>$1000) could not be loaded into the memory due to their excessively large size, so that the direct MIP approach was not viable. On the other hand, the proposed BD(ϵ) with $\epsilon > 0$ shows better performance than the direct MIP approach even if the size is small except for the case of 24^1. For the large-sized instances, it was 4 to 16 times faster than BD(0). Furthermore, Table VIII shows that even though the controllable parameter ϵ increases, the expected cost increases much smaller, which is also significantly smaller than that of reactive policies. This shows that the proposed decomposition algorithm with the controllable parameter can find near-optimal solutions in much less time.

2) Different Numbers of Generators: The computational time of the proposed algorithm is also compared to the direct MIP approach for the different number of generators. The 8-unit data is generated by dividing the min-max capacity, the ramp rate, and the start-up cost of each generator in Table I by half. For each number of generators, five instances were also generated with the same islanding probabilities as described in Section IV-D1. The average computation time over five instances for each solution approach when $T = 24$ and $\tau = 2$ is shown in Fig. 8. The result demonstrates that the BD(0) is more sensitive to the number of generators than the others. In other words, more iterations are needed to converge with the proposed decomposition approach. On the other hand, the computational times of the other approaches with the 8-unit instance increased at a similar rate. In other words, we can still obtain a high-quality solution in a reasonable time, by using BD(ϵ) controlling $\epsilon > 0$.

E. A heuristic based on the T^1 criterion

One possible way to set up a feasible operation plan for the T^τ criterion is to apply the T^1 criterion repeatedly. To test the effectiveness of this approach, we devised and tested a heuristic which we call a *recursive T^1 criterion*: solve a model with T^1 to set up a baseline operation plan, and when an

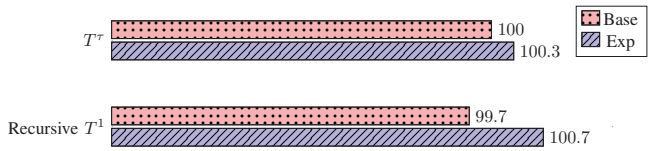

Fig. 9. Cost comparison of T^τ and the recursive T^1 in $T = 24$ and $\tau = 2$

islanding occurs at $t^{'}$, another T^1 is solved to amend the plan from $t^{'}$ onward. The baseline operation costs and the expected costs for the whole scenarios are compared in a environment where $T = 24$ and $\tau = 2$, as described in the Section IV-B1, and all costs were scaled by setting the base cost of the T^τ criterion (USD 15,900) to 100. The islanding probability was also set to 0.1, and the probability of the islanding scenario in the heuristic ($p_i^{'}$ for $i \in H$) was set to the sum of the islanding scenarios that the first islanding occurs at i in T^τ; i.e. $p_i^{'} := \sum_{s \in S_i} p^s$. Fig. 9 shows that in comparison to T^τ criterion, the baseline plan's cost of the heuristic is lower, the expected cost of the heuristic is higher, and there is little difference between the costs. In addition, the expected cost of the heuristic is less than those of reactive policies, which has shown in Table IV given earlier. This result implies that the MGO can apply a recursive T^1 criterion as a heuristic to operate a microgrid as an alternative to T^τ criterion.

V. Conclusion

This study proposes a novel systematic method to optimize a proactive policy for the operation of microgrids under the possibility of islanding events from the MGO's point of view. Based on the T^τ criterion that considers recurring multi-period islanding events, a multistage stochastic optimization model is proposed. This model carefully considers the non-anticipativity constraint that establishes the executable operation plans. To deal with the large-scale optimization model, an efficient decomposition algorithm is also devised. Computational experiments show that the proposed proactive policy significantly reduces the expected operation costs as well as the worst-case cost scenario. In addition, it is robust to the changes in the market prices in comparison to the reactive policies. Therefore, the proposed approach can be practically used to reliably and cost effectively operate microgrids under islanding uncertainty. It can also help the MGOs participating in the reserve market to establish their own bidding strategy. In addition, it can be applied to other situations other than island operations, in which the system's condition changes discretely and repeatedly during the planning horizon (e.g. generation scheduling under network reconfigurations). For further directions to implement the proposed method in practice, a probability distribution of the islanding events needs to be estimated more precisely based on the market environment in which the reserve resources are deployed and used. In addition, further studies are required that considers the MGO's compensation when the system operator activates the islanded operation as a reserve resource. Finally, along with the islanding uncertainty, other various uncertain factors, such as the electricity price, demand, and renewable generation, can be considered in future research. Since this would mean that a large number of scenarios in a multi-stage program would have to be considered, an efficient method to mitigate the computational burden should be studied.

References

[1] F. Katiraei, R. Iravani, N. Hatziargyriou, and A. Dimeas, "Microgrids management," *IEEE Power and Energy Magazine*, vol. 6, no. 3, pp. 54–65, 2008.

[2] J. Mitra and M. R. Vallem, "Determination of storage required to meet reliability guarantees on island-capable microgrids with intermittent sources," *IEEE Transactions on Power Systems*, vol. 27, no. 4, pp. 2360–2367, 2012.

[3] C. Gouveia, J. Moreira, C. L. Moreira, and J. A. Pecas Lopes, "Coordinating storage and demand response for microgrid emergency operation," *IEEE Transactions on Smart Grid*, vol. 4, no. 4, pp. 1898–1908, 2013.

[4] S.-J. Ahn and S.-I. Moon, "Economic scheduling of distributed generators in a microgrid considering various constraints," in *2009 IEEE Power & Energy Society General Meeting*, pp. 1–6, IEEE, 2009.

[5] H. Farzin, M. Fotuhi-Firuzabad, and M. Moeini-Aghtaie, "Stochastic energy management of microgrids during unscheduled islanding period," *IEEE Transactions on Industrial Informatics*, vol. 13, no. 3, pp. 1079–1087, 2017.

[6] A. Khodaei, "Microgrid optimal scheduling with multi-period islanding constraints," *IEEE Transactions on Power Systems*, vol. 29, no. 3, pp. 1383–1392, 2014.

[7] A. Khodaei, "Resiliency-oriented microgrid optimal scheduling," *IEEE Transactions on Smart Grid*, vol. 5, no. 4, pp. 1584–1591, 2014.

[8] A. Gholami, T. Shekari, F. Aminifar, and M. Shahidehpour, "Microgrid scheduling with uncertainty: The quest for resilience," *IEEE Transactions on Smart Grid*, vol. 7, no. 6, pp. 2849–2858, 2016.

[9] M. Vahedipour-Dahraie, H. Rashidizadeh-Kermani, A. Anvari-Moghaddam, and P. Siano, "Flexible stochastic scheduling of microgrids with islanding operation complemented by optimal offering strategies," *CSEE Journal of Power and Energy Systems*, 2020.

[10] Y. Guo and C. Zhao, "Islanding-aware robust energy management for microgrids," *IEEE Transactions on Smart Grid*, vol. 9, no. 2, pp. 1301–1309, 2018.

[11] A. Gholami, T. Shekari, and S. Grijalva, "Proactive management of microgrids for resiliency enhancement: An adaptive robust approach," *IEEE Transactions on Sustainable Energy*, vol. 10, no. 1, pp. 470–480, 2019.

[12] F. Aminifar, M. Fotuhi-Firuzabad, and M. Shahidehpour, "Unit commitment with probabilistic spinning reserve and interruptible load considerations," *IEEE Transactions on Power Systems*, vol. 24, no. 1, pp. 388–397, 2009.

[13] Q. Zhang, M. F. Morari, I. E. Grossmann, A. Sundaramoorthy, and J. M. Pinto, "An adjustable robust optimization approach to scheduling of continuous industrial processes providing interruptible load," *Computers & Chemical Engineering*, vol. 86, pp. 106–119, 2016.

[14] K. Bhattacharya, "Interruptible load management within secondary reserve ancillary service market," in *Power Tech Proceedings, 2001 IEEE Porto*, vol. 1, pp. 1–6, IEEE, 2001.

[15] J. H. Eto, J. Nelson-Hoffman, C. Torres, S. Hirth, B. Yinger, J. Kueck, B. Kirby, C. Bernier, R. Wright, A. Barat, *et al.*, "Demand response spinning reserve demonstration," tech. rep., Ernest Orlando Lawrence Berkeley NationalLaboratory, Berkeley, CA (US), 2007.

[16] S. Y. Lee, Y. G. Jin, and Y. T. Yoon, "Determining the optimal reserve capacity in a microgrid with islanded operation," *IEEE Transactions on Power Systems*, vol. 31, no. 2, pp. 1369–1376, 2016.

[17] E. Ela, M. Milligan, A. Bloom, A. Botterud, A. Townsend, and T. Levin, "Evolution of wholesale electricity market design with increasing levels of renewable generation," tech. rep., National Renewable Energy Lab.(NREL), Golden, CO (US), 2014.

[18] A. Anisie, E. Ocenic, and F. Boshell, "Innovation landscape brief: Increasing time granularity in electricity markets," tech. rep., International Renewable Energy Agency, 2019.

[19] Á. Lorca, X. A. Sun, E. Litvinov, and T. Zheng, "Multistage adaptive robust optimization for the unit commitment problem," *Operations Research*, vol. 64, no. 1, pp. 32–51, 2016.

[20] Q. P. Zheng, J. Wang, P. M. Pardalos, and Y. Guan, "A decomposition approach to the two-stage stochastic unit commitment problem," *Annals of Operations Research*, vol. 210, no. 1, pp. 387–410, 2013.

[21] J. F. Benders, "Partitioning procedures for solving mixed-variables programming problems," *Numerische Mathematik*, vol. 4, no. 1, pp. 238–252, 1962.
[22] J. R. Birge and F. Louveaux, *Introduction to Stochastic Programming*. Springer Science & Business Media, 2011.
[23] S. Kazarlis, A. Bakirtzis, and V. Petridis, "A genetic algorithm solution to the unit commitment problem," *IEEE Transactions on Power Systems*, vol. 11, no. 1, pp. 83–92, 1996.
[24] Historical Load Forecast, PJM. [Online], 2018. https://dataminer2.pjm.com/feed/load_frcstd_hist/definition.
[25] A. Papavasiliou and S. S. Oren, "Multiarea stochastic unit commitment for high wind penetration in a transmission constrained network," *Operations Research*, vol. 61, no. 3, pp. 578–592, 2013.
[26] J. Frayer, S. Keane, and J. Ng, "Estimating the value of lost load," *London Economics International LLC*, 2013.
[27] FICO® Xpress Optimization. [Online], 2020. https://www.fico.com/.
[28] E. Nicholson, "Operator-initiated commitments in RTO and ISO markets," tech. rep., FERC, 2014.

Jongheon Lee (S'20) received the B.S. and M.S. degrees in industrial engineering from Seoul National University, Seoul, Korea, in 2017 and 2019, respectively. Currently, he is pursuing the Ph.D. degree in the Department of Industrial Engineering, Seoul National University, Seoul, Korea. His research interests include large-scale and stochastic optimization with application in energy systems.

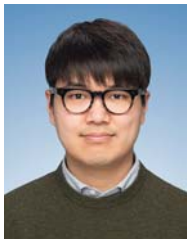

Siyoung Lee (M'17) received the B.S., M.S., and Ph.D degrees in electrical engineering from Seoul National University, Seoul, Korea, in 2009, 2011, and 2016, respectively.

From 2017, he has been an Assistant Professor with the Department of Energy and Electrical Engineering, Korea Polytechnic University. His research interests include electric power market design and operation considering the integration of distributed energy resources in the distribution system and the P2P trades among them.

Kyungsik Lee (M'17) received the B.S. degree in industrial engineering in 1993 from Seoul National University, Seoul, Korea. He also received the M.S. and Ph.D degrees in industrial engineering from Korea Advanced Institute of Science and Technology, Daejeon, Korea, in 1995 and 1998, respectively.

He is a Professor of Industrial Engineering and Associate Director of the Institute of Industrial Systems Innovation at Seoul National University. His teaching and research interests include large-scale optimization modeling and algorithms, including their application in manufacturing, transportation and logistics, and energy systems.